Nature Environment and Pollution Technology
An International Quarterly Scientific Journal

p-ISSN: 0972-6268
(Print copies up to 2016)
e-ISSN: 2395-3454

Vol. 21 | No. 3 | pp. 1279-1288 | 2022

Original Research Paper

https://doi.org/10.46488/NEPT.2022.v21i03.034

Open Access Journal

Application of Geo-electrical Methods for Estimating Water Infiltration in Soils

Kaizar Hossain*, Mohd Talha Anees†, Ahmad Farid Bin Abu Baker**, Mohammad Muqtada Ali Khan***, Amin E. Khalil****, K. S. Ishola*****, Abdullah K.******, Mohd Nawawi M. N.****** and Mohd. Omar A. K.*******

*Department of Environmental Science, Asutosh College, University of Calcutta, Shyamaprasad Mukherjee Road, Kolkata-700 026, West Bengal, India

**Department of Geology, Faculty of Science, University of Malaya, Kuala Lumpur 50603, Malaysia

***Faculty of Earth Science, Universiti Malaysia Kelantan, Jeli Campus, 17600 Jeli, Kelantan, Malaysia

****Department of Geology, Faculty of Science, Helwan University, Helwan, Greater Cairo 11795, Egypt

*****Department of Geosciences, University of Lagos, Akoka, Lagos, Nigeria

******Geophysics Section, School of Physics, Universiti Sains Malaysia, Minden 11800, Penang, Malaysia

*******School of Industrial Technology, Universiti Sains Malaysia, Minden 11800, Penang, Malaysia

†Corresponding author: Mohd Talha Anees; talhaanees_alg@yahoo.in

Nat. Env. & Poll. Tech.
Website: www.neptjournal.com

Received: 21-08-2021
Revised: 04-10-2021
Accepted: 26-10-2021

Key Words:
Electrical resistivity tomography
Hydraulic conductivity
Infiltration rate
Permeability
Transient electromagnetic

ABSTRACT

In this study, an alternative approach was applied for the characterization of the subsurface geological conditions to estimate the hydrological parameters in the absence of subsurface soil data. The study revealed that the hydrological parameters, estimated from the Transient Electromagnetic (TEM) and Electrical Resistivity Tomography (ERT), were significantly correlated with in situ data. Overall estimated infiltration rate (below 20 inches/h) predicted fine-grained soil was also associated with in situ data. A high correlation among the bulk electrical resistivity, porosity, and the resistivity of the pore fluid thereby confirmed the relevance of Archie's law used in this study. Furthermore, results showed that both TEM and ERT are vital tools for hydrological parameter estimation.

Soil water infiltration is a significant part of the hydrological cycle (Todd & Mays 1980). It depends on the distribution of subsurface soil texture and structure, which maintains soil moisture conditions. Infiltration in unconsolidated soils is proportional to grain size and distribution (Cui et al. 2017). While the infiltration in the clayey soil is slow because of the small grain size and high resistance to water movement. The spatial variability of soil structure is determined by soil profile observations and soil properties measurements such as bulk density and porosity. The tools available for the investigation of water movement in the soil are limited to a specific point measurement and are destructive, whereas the geophysical methods are usually non-invasive. They disturb neither the structure nor the water dynamics of the soil (Michot et al. 2003).

Infiltration rate can be measured using in-situ methods such as the double-ring method (Shaari et al. 2016, Fatehnia et al. 2016) and laboratory experiments (Morbidelli et al. 2015). However, it is difficult to carry out experiments in high-relief areas due to slope steepness and logistic handling. Alternatively, geophysical methods are cost and time-effective methods for the proper assessment of subsurface soil parameters. As the soil's electrical conductivity varies due to the presence of pore water, saltwater, and temperature, electrical resistivity methods will be helpful to estimate subsurface hydrological factors such as hydraulic conductivity, porosity, and permeability (Anees et al. 2017).

In previous studies, electrical resistivity techniques have been used for different purposes such as groundwater developments (Kumar et al. 2016, Afshar et al. 2015), water distribution in landfills (Dumont et al. 2016), landslide investigation (Perrone et al. 2014), monitoring of seasonal water content variations (Chrétien et al. 2014, Brunet et al. 2010), porosity or hydraulic conductivity estimation (Chou et al. 2016, Niwas & Celik 2012, Ghose & Slob 2006) and infiltration estimation (Crosbie et al. 2014). Some of these studies used a variety of electrical resistivity techniques, such as electrical resistivity tomography (ERT), vertical electri-

cal sounding (VES), and time-domain-induced polarization (TDIP). Transient electromagnetic (TEM) is a geophysical method often used for subsurface hydrogeological mapping (Danielsen et al. 2003, Al-Garni & El-Kaliouby 2011). In the case of shallow depth investigations (up to a depth of 100 m), the instrumental setup of TEM is short and easy as compared to the other resistivity methods, which make it useful for a survey, especially in hilly terrain (Danielsen et al. 2003, Flores et al. 2013). TEM is the right technique for an accurate determination of the bulk resistivity of the subsurface geological units. In some situations, such as rough topography or limited space, lying down transmitter loops become difficult. In such cases, resistivity imaging techniques come to the rescue. Resistivity imaging is also given preference in those areas where the distribution of resistivity is multi-dimensional.

Electrical resistivity methods have been used to estimate the infiltration rate from empirical relationships (Noell et al. 2011, Chou et al. 2016). However, none of the studies have related the electrical resistivity and infiltration rate to flooding, which developed the motivation to conduct this study. The conventional methods to estimate the infiltration rate are based on the point or one-dimensional measurement. Whereas, in flood-related studies, two to three-dimensional measurements are required for accurate results. During flooding, the infiltration rate becomes slow as the large load of suspended particles quickly forms a clogging layer (Chen et al. 2013). Because of this, a shallow depth investigation should be enough to conduct infiltration rate measurement. Therefore, this study has two main purposes. The first is to estimate or identify soil-related parameters for empirical equations to estimate subsurface hydrological parameters. The second is the use of ERT and TEM to estimate the two-dimensional subsurface infiltration rate.

The main aim of this study was to characterize the spatial variability of soil structure in the hilly terrain of Kelantan State, Malaysia, using both TEM and ERT. The specific objectives were (i) to carry out in-situ subsurface resistivity distribution in terms of lateral and vertical variations in the resistivity values, (ii) to estimate soil parameters from empirical relationships in a data-sparse environment, and (iii) to develop multilayer regression models for the study area to know the accuracy of the estimated soil parameters and (iv) to validate the TEM and the ERT outputs with borehole and in situ data. The alternative approach of this study in the absence of soil parameter data will be helpful to estimate the multi-dimensional infiltration rate for flood vulnerability and risk analysis.

MATERIALS AND METHODS

Location and Details of the Study Area

The location of the study area is in Kelantan State, the north-eastern part of Peninsular Malaysia. It lies between Latitudes 4°33'N and 6°14' N, longitudes 101°19'E and 102°39'E with an area of approximately 15000 km^2. The elevation ranges from 0 to 2.2 km above mean sea level. The slope varies from 0 to 89 degrees. Sungai Kelantan is the main river, which divides approximately 107 km into Sungai Galas and Sungai Lebir (Fig. 1).

The climate is tropical, and humid with an average temperature range from 20 °C to 30 °C. The average annual rainfall is 3017 mm, and the average daily wind speed is 1.50 $m.s^{-1}$. The regional geology of Kelantan consists of sedimentary and metasedimentary rocks in the central zone, while granite is situated on the eastern and western borders of the Boundary Range and Main Range respectively (Heng et al. 2006). According to the Department of Agriculture, Malaysia, there are 21 soil series in the catchment. But the area is dominated by three such as steep land (63.9%) followed by Durian-Munchong-Bungor (14.3%) and Rengam-Jerangau (5.4%). The eastern and western mountain ranges have a granitic soil cover that is composed of fine to coarse sand and clay. The minimum depth of soil cover is a meter on steep land, while the depths increase up to 18 m downstream. A fine sandy loam soil up to a few meters is found on the steep slope of the basin. At mid and downstream, a clay layer of an average depth of 4 m is situated. Also, there is a layer of fine to medium-grained sand in a few places. The depth of the clay layer decreases near the sea downstream while the depth of the fine to medium-grained sand layer increases.

Data Acquisition

Electrical resistivities were measured through thirteen profiles of TEM and nine profiles of ERT surveys that covered upstream, midstream, and downstream of the study area. Survey locations were mostly on the river bank to know the infiltration rate, which is essential in floodplain hydrological modeling. TEM data were collected using a terra team Monex GeoScope instrument with a current of 5 A and 12 V batteries. The stacking time was set to 3 minutes with a 50 Hz noise filter to remove interference from the power lines. TEM profiles were in the form of loops. Each loop was 20 m × 10 m in dimension, which have eight 5 m × 5 m small loops to get high-resolution data (Fig. 2).

ERT data were collected through a 100 m profile at nine locations using the ABEM Terrameter system. The system had an automatic switch box and an array of 41 metal stake electrodes at 2.5 m electrode spacing. The Wenner-Schlumberger electrode spacing was used that allows measurements up to a depth of 40 m depth was used.

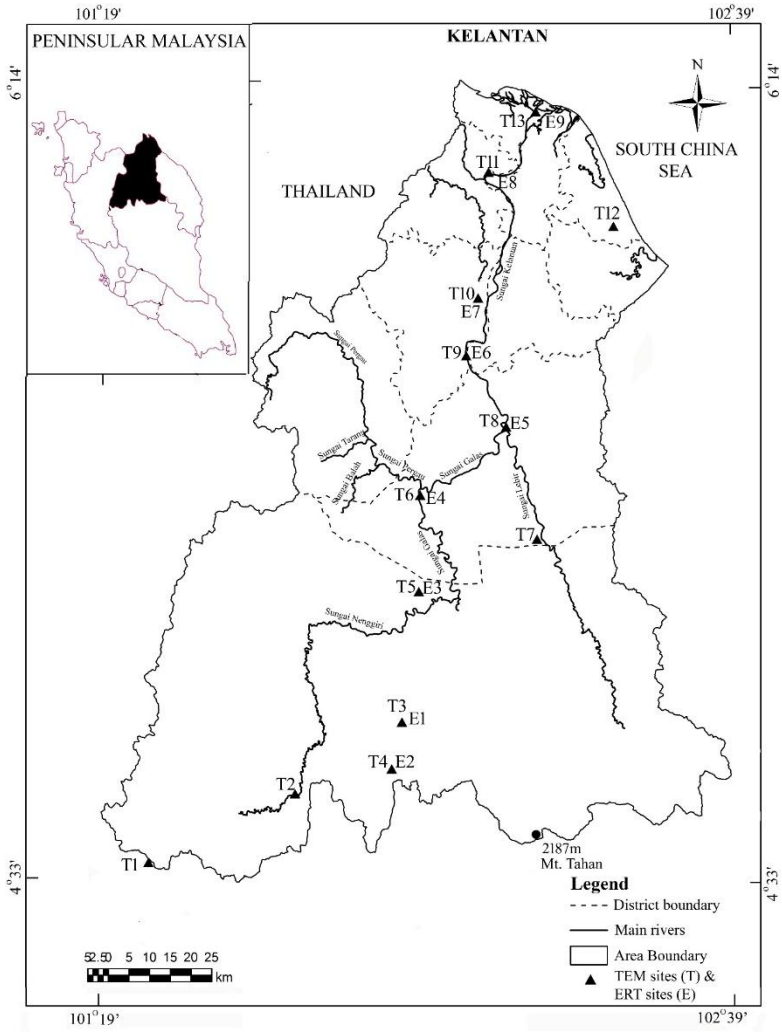

Fig. 1: Location of TEM and ERT sites in the study area.

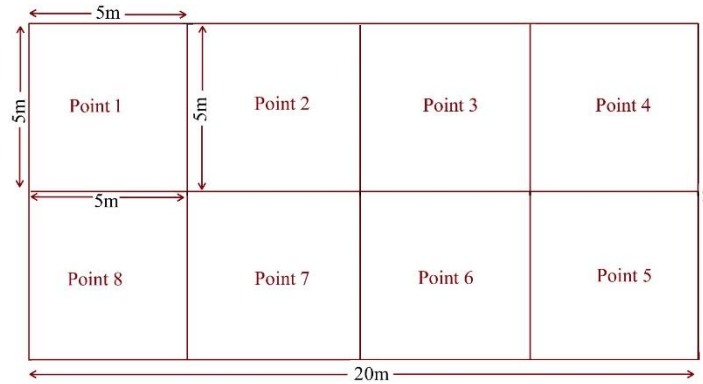

Fig. 2: TEM profiling with 5m-by-5m loop.

In-situ Soil Sampling

In-situ soil samples with 20 cm depth were collected at thirteen locations. These samples were brought back to the laboratory, air-dried, and sieved through a 2 mm sieve. A hydrometer test was used to calculate the amount of sand, silt, and clay (Bouyoucos 1962). In addition, for results validation, the log data was collected from the Department of Mineral and Geoscience, Malaysia.

Calculation of Porosity

For porosity calculation, the most widely used Archie's equation (Archie 1942) for electrical resistivity was selected, which is given as:

$$\rho = a\rho_w \emptyset^{-m} \quad \ldots(1)$$

where ρ and ρ_w are bulk resistivity of rock or unconsolidated soil and resistivity of pore fluid in Ωm respectively, Ø is the porosity of aquifer, a is the electrical tortuosity parameter, and m is the cementation factor. Eq. (1) is not valid for silt and clay because it only captures pore water conduction. It needs some modification for silt and clay. Therefore, the calculation of the cementation factor was by the equation (Choo et al. 2016):

$$m = m_{sand}.(1 - VF_c) + m_{clay}.VF_c \quad \ldots(2)$$

where m_{sand} and m_{clay} are the cementation factors for pure sand and pure clay respectively. VFc is the volume fraction of clay. The cementation factor was calculated for each site based on the clay percentage from Eq. (2). Pure sand and pure clay values were used at 1.55 and 2.11 respectively to modify the cementation factor (Choo et al. 2016). The cementation values vary from 1.58 (site number 11) to 1.74 (site number 3). As these cementation values were based on the 20 cm depth and it may not be the same as up to 20 m depth. Therefore, the average value of 1.66 was selected for the entire study area.

The electrical tortuosity parameter (a), which is related to the path length of the current flow, is almost unity for unconsolidated sediments (Niwas & Celik 2012). Hence, a = 1 was used for this study. Generally, pore fluid resistivity (ρ_w) values are measured from laboratory experiments. Due to the lack of this data, the ρ_w values for different ρ were collected from previous studies. Based on Niwas and Celik (2012) and Choo et al. (2016) studies, ρ_w values for different bulk resistivity were identified, which are given in Table 1.

Calculation of Permeability

Kozeny (1953) developed a relationship between porosity and intrinsic permeability, which is given as:

$$k = \frac{d^2}{180}\frac{\emptyset^3}{(1-\emptyset)^2} \quad \ldots(3)$$

where k is intrinsic permeability, and d is grain size in a meter. Subsurface grain size data of different soil types were obtained from the literature. Based on the porosity values (from Eq. 1), the soil texture classification was identified through the United States Department of Agriculture (USDA) textural classification (Maidment 1993) and Geotechdata.info (2013). Medium particle diameter (d50) values were obtained from the United States Environmental Protection Agency (US EPA) Geotechnical Particle Size and Soil Classification Table (US EPA).

Calculation of Hydraulic Conductivity and Infiltration Rate

The hydraulic conductivity was calculated from the equation used by Niwas and Celik (2012) whereas, for infiltration rate (I), the Green-Ampt infiltration model using Darcy's law was selected, which is given as (Green and Ampt 1911):

$$I = \frac{dF}{dt} = K\left[1 + \frac{M\varphi}{F}\right] \quad \ldots(4)$$

where M is the water content in the soil layer and F is the total infiltrated volume between the surface of the soil and the wetting front, which can be calculated as:

$$F = M \times D \quad \ldots(5)$$

where D is cumulative infiltration depth. φ is the capillary pressure at the wetting front, which can be calculated by the equation (Morel-Seytoux et al. 1996):

$$\varphi = \frac{0.046\beta + 2.07\beta^2 + 19.5\beta^3}{(1 + 4.7\beta + 16\beta^2)\alpha} \quad \ldots(6)$$

where α and β are van Genuchten-Mualem parameters (Van Genuchten 1980). The van Genuchten-Mualem parameters α and β are needed to calculate the capillary pressure at the wetting front (φ), which were obtained from previous studies (Bohne et al. 1989, Chen et al. 2015).

Table 1: Pore water resistivity values for different ranges of bulk resistivity values for this study.

Bulk resistivity (ρ) (Ωm)	Pore water resistivity (ρ_w) (Ωm)
0.5-5	0.49
5-20	4.3
20-100	11.1
100-200	14.9
200-500	20.6
>500	77

Regression Model and Validation

Linear regression was used to obtain the empirical relationships between bulk resistivity and pore water resistivity, bulk resistivity and porosity, and porosity and grain size. The borehole data was used to validate the TEM and ERT results. Infiltration rate (I) was validated using previous studies' results in the same study area (Shaari et al. 2016). They used the double ring method (up to 60 cm depth) to observe infiltration capacity at seven places in the Kota Bharu District, where sites numbers 13 and 11 of this study were located.

Comparison of TEM and ERT Outputs

Direct comparison of the resistivity values from TEM and ERT is not possible because of their different mechanism for measuring the resistivity values. TEM produces eddy currents while the ERT produces direct currents (Firdaus 2018). However, a comparison of output patterns of TEM and ERT is possibly used in this study.

RESULTS AND DISCUSSION

Results of TEM and ERT Inversion Models

For this study, 20 m depth was selected due to the formation of clogging layers since the infiltration depth during flooding is low. For TEM, out of 13 places, the upper layer resistivity values of 11 locations ranged from 24 Ωm to 80 Ωm, which indicates that the upper layers were mostly fine soil, such as silt and clay with available water as the absorption water (Saarenketo 1998). Whereas, at the other two sites of TEM, identification of the upper layers were as clayey soil (160 Ωm) and clayey sand (460 Ωm) (Eluwole et al. 2018). For ERT, the upper layers of 6 locations were mostly a mixture of sand and clay. While at the rest of the three locations, silt and clay content were dominating. Overall, the average resistivity values of the upper layers ranged from 98 Ωm to 1421 Ωm, which indicates the presence of loamy soil (Eluwole et al. 2018). The overall results showed that the prediction of the output of both TEM and ERT was sand, silt, and clay content in the upper layer of soil.

Porosity (∅)

Results of the hydrometer analysis indicated that an average of 28% sand, 52% silt, and 20% clay were present at 20 cm depth, with approximately 6% of organic matter at all the locations. Based on these compositions, the study area is characterized by silty loam soil (Vaezi et al. 2016). The average porosities of the top layers (0 to 5m depth) were 0.24 (TEM) and 0.25 (ERT), which indicates the presence of silty sands (Das 2013). It shows closer prediction by both the techniques. Also, the variation in porosity shows a mixture of clay and fine sand (Geotechdata.info 2013).

Intrinsic Permeability (k) and Hydraulic Conductivity (K)

The results of soil texture classification, ranges of porosity, and medium particle diameter (d_{50}) obtained from the literature are shown in Table 2.

The intrinsic permeability values ranged between 10^{-10} to 10^{-11} m^2. It indicates that the soil in the study area is semi-permeable (Bear1972), and it is dominant in silt and clay content at all the sites. As mentioned above, the study area is characterized by silty loam soil, which contains 70% silt and clay and 20% sand. It shows the distribution of small grain size and slow permeability in the silty loam soil (Shepherd 1989). TEM and ERT predicted accurate permeability values at all the sites except site number 13 in ERT. The top layer at site 13 is showing high resistivity values, which predict high porosity and hence high permeability (8.54×10^{-11} m^2).

The hydraulic conductivity (K) values ranged from 10^{-4} to 10^{-8} $m.s^{-1}$, which represents fine sand, silt, loess, and loam (Bear 1972, Freeze & Cherry 1979). The K values for TEM and ERT up to 5m depth were ranged from 0.12×10^{-5} m/s to 8.98×10^{-5} m/s and 0.36×10^{-5} m/s to 8.04×10^{-5} m/s respectively. The average K values up to 20 m depth for TEM and ERT were estimated as 3.48×10^{-5} m/s and 5.16×10^{-5} m/s respectively. These values showed the dominancy of silt and clay in subsurface soil, which makes it less permeable. These results conformed with the intrinsic permeability. Here also, K values at site 13 were high, which showed high sand content as compared to other sites.

Infiltration Rate (I)

The infiltration rate values predicted by TEM and ERT varied from 10-4 to 10-6 m/s in all the layers. If the conversion of these infiltration values is into inch per hour, then all the values lay under 20 inches/h except at site 13, which showed the presence of sandy loam to clay content in subsurface soil (Brouwer et al. 1988). The average infiltration rate predicted by the TEM showed clayey soil, while ERT predicted clay loam up to 20 m depth. At site 13, the infiltration rate was predicted by TEM showed clayey soil whereas, ERT showed a mixture of sand and clay loam. The higher infiltration rate predicted by the ERT at this site varied from 5m to 15m depth and 0 to 10 m distance. Other parts of this site were represented by the clay loam.

Regression Models

The content of fines in soil has a proportional influence on its bulk resistivity. It means that soil with a relatively higher

Table 2: Identified soil texture classification based on porosity and identified medium grain size based on soil texture classification for this study. van Genuchten-Mualem parameters α and β to calculate the capillary pressure at the wetting front (φ) for this study.

Texture classification	Porosity range		Medium grain size (d_{50}) (mm)	α	β
	Minimum	Maximum			
Sand	0.233	0.268	0.29	14.5	0.626
well graded sand	0.215	0.426	0.36	3.63	0.669
sandy gravel	0.21	0.32	0.22	3.63	0.669
Sandy loam	0.447		0.15	4.4	0.137
Sandy clay loam	0.398	0.400	0.14	5.9	0.324
Loamy sand	0.435	0.444	0.41	5.35	0.249
Loam	0.285	0.470	0.027	5.37	0.118
Silty sand	0.21	0.49	0.18	0.44	0.242
Silt loam	0.494	0.562	0.021	0.379	0.165
Silty or sandy clay	0.201	0.607	0.0067	0.095	0.153
silty/clayey fine sand	0.540	0.549	0.0147	1.5	0.588
Silt	0.515	0.526	0.0038	0.379	0.165
Silty clay	0.333	0.635	0.0024	0.479	0.152
Organic Silty clay	0.575	0.579	0.0024	0.479	0.152
Clayey sandy gravel	0.178	0.187	0.215	2.76	0.539
Clayey sand	0.15	0.37	0.14	2.205	0.588
Clay	0.472	0.475	0.0027	0.479	0.152

content of fines will have a higher bulk resistivity (Fig. 3b).

The Association of high values of porosity was with soils having a small amount of fines content. High porosity indicated the dominance of larger sand grains (Fig. 3c and 3d) (Li & Sherman 2015). Variations of porosity with grain size for both TEM and ERT are shown in Fig. 3 (e and f), where the porosity tends to decrease for soils with increasing grain size and then increases as the grain size decreases. The decline in the porosity values could result from an increment in the number of clay particles, which gradually filled the void spaces (Cameron & Buchan 2017) and separated the relatively bigger sand particles, thus, becoming the loading-bearing unit of the soil.

Validation of TEM and ERT Models

From the available well log data, two well logs (named BH 1 and BH 2) were found near the two sites and selected for comparison. The exact locations of BH 1 (6 m deep) were at site 13, whereas BH 2 (17 m deep) was sited 1.7 km from site number 11. The comparison of resistivity values from TEM and ERT with well-log data was based on the resistivity chart proposed by Palacky (1988).

In borehole BH1, the top layer of 1.2 m is made up of soft clay with some sand sediments. Below 1.2 m depth, sand sediments increase in size with slightly clayey sediments to a depth of 4.2 m. Soft clay is again encountered at a depth between 4.2 m and 6.0 m, where the drilling terminated. At this site, from the TEM measurements, the bulk resistivity values were 30.7 Ωm (0 to 5 m depth), 30.7 Ωm (5 to 10 m depth), 23.8 Ωm (10 to 15 m depth), and 12.2 Ωm (15 to 20 m depth). The geological interpretation of these low resistivity values indicated the presence of clayey soil. At the same place and the same depth, the bulk resistivity values from ERT measurements were 82.9 Ωm, 38.3 Ωm, 56.8 Ωm, and 68.7 Ωm (Fig. 4).

In borehole log BH2, the first lithologic unit of this layer encountered at the depth of 1.8 m is clay sediment. This sediment (considered the second layer) extends to about 6 m in depth and is made of clay with some fine and medium-grained sand. The third layer (4.6 m deep) is of clay with some fine-grained sand, while the fourth layer (0.9 m deep) is of fine-grained sand with some clay. The fifth layer is encountered at depth of 1.3 m deep is of medium-grained sand with some clayey sediments. The last geological material encountered at depth of 2.2 m is clayey sediments. From the TEM survey, the bulk resistivity values for four layers were 23.5 Ωm, 23.6 Ωm, 41.9 Ωm, and 41.9 Ωm respectively, which indicated the clayey soil. Whereas from the ERT survey, the bulk resistivity values

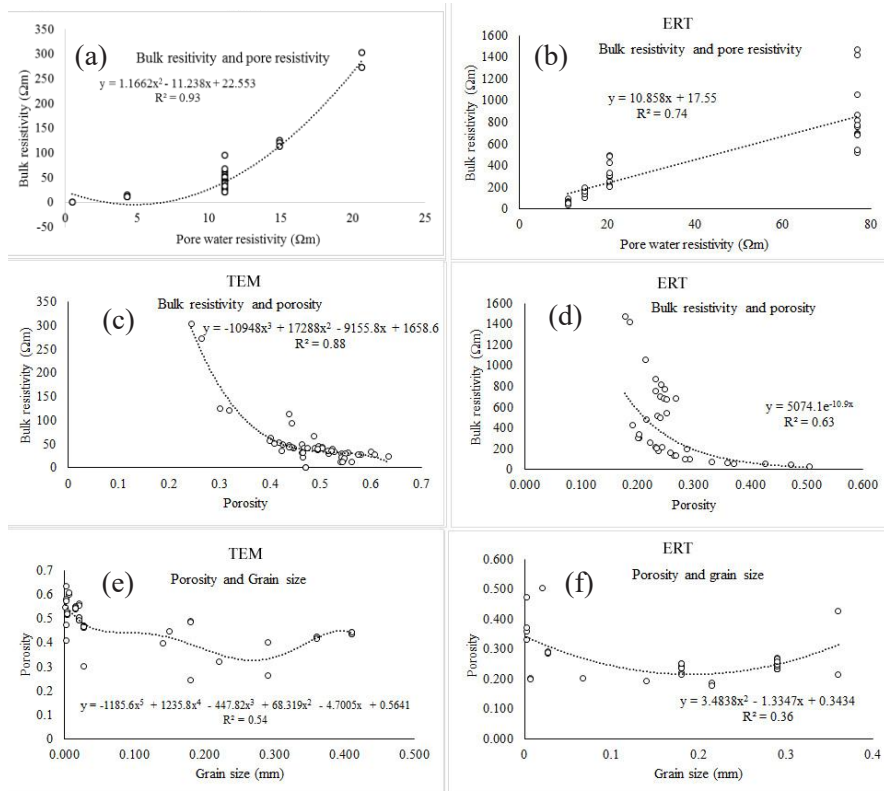

Fig. 3: Regression models (a) for bulk resistivity and pore water resistivity for TEM (b) for bulk resistivity and pore water resistivity for ERT (c) bulk resistivity and porosity for TEM (d) bulk resistivity and porosity for ERT (e) porosity and grain size for TEM (f) porosity and grain size for ERT.

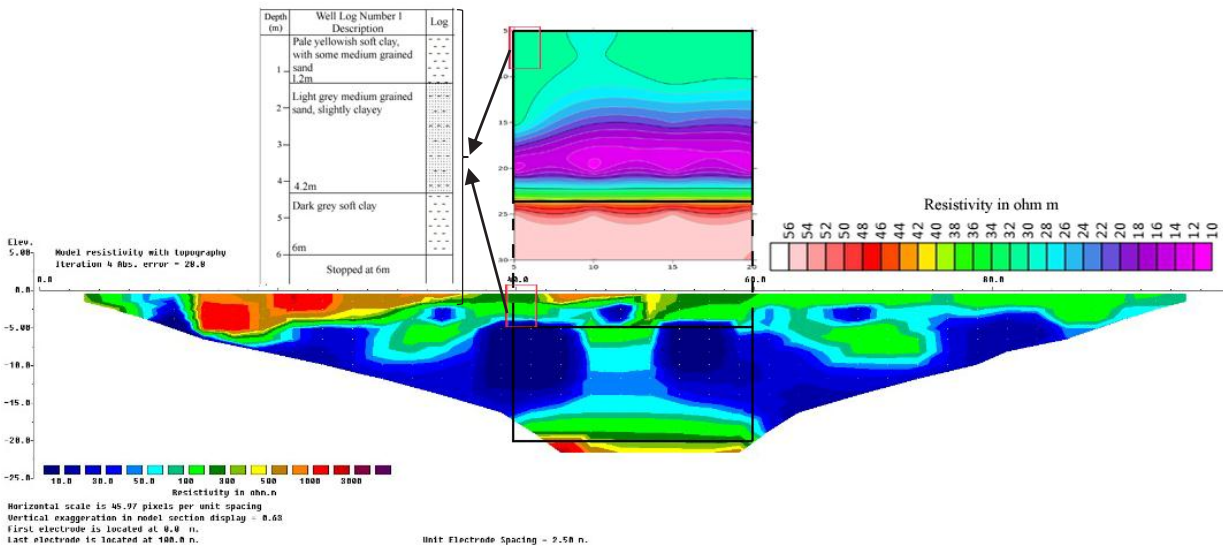

Fig. 4: Validation of TEM and ERT outputs with borehole data at site number 13.

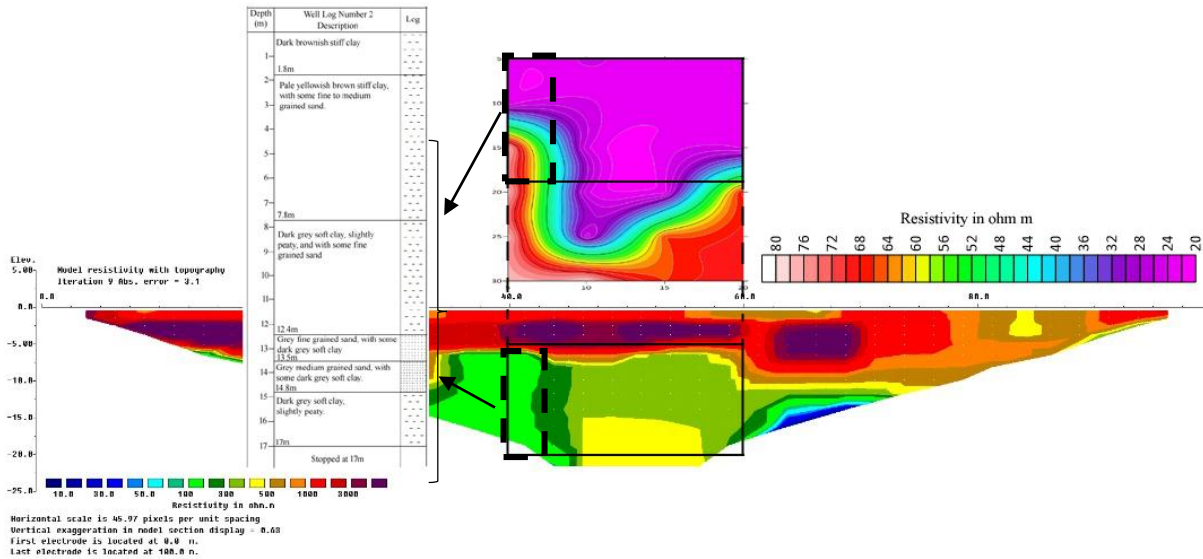

Fig. 5: Validation of TEM and ERT outputs with borehole data at site number 11.

were 1881.3 Ωm, 1503.9 Ωm, 1110.1 Ωm, and 1110.1 Ωm respectively.

These layers show the medium-grained sand at the top while fine-grained sand is below 5m depth. The borehole log data shows a mixture of fine and medium-grained sand with clay content in almost all layers (Fig. 5).

The observed infiltration capacity varies from 13.20 $mm.h^{-1}$ to 206.3 $mm.h^{-1}$. For the upper layer, the estimated I at sites 11 and 13 for TEM were 15.09 $mm.h^{-1}$ and 61.83 $mm.h^{-1}$ respectively, while for ERT, the estimated I were 12.93 $mm.h^{-1}$ and 253.95 $mm.h^{-1}$ for sites 11 and 13 respectively. It was observed that the estimated I for TEM and ERT at both sites lies within the range of the observed infiltration capacity (Shaari et al. 2016). It should be noted here that sites number 11 and 13 are not exactly at the same place as the observed infiltration rate. Therefore, the range of the infiltration rate was considered for the validation. Hence, it can be concluded that both the techniques overall worked well in the estimation of the hydrological parameters. Also, because of the different types of currents used in TEM and ERT, the estimations were not exactly matched but have some range of the hydrological parameters.

CONCLUSIONS

The results showed that, for TEM, the bulk resistivity was less than 80 Ωm, while for the ERT it was 1421 Ωm. This range was predicted by the mixture of sand, silt, and clay content in which silt and clay were dominating whereas the average prediction was clayey soil for TEM and loamy soil for ERT. The porosity range by both the techniques showed closer estimation with in situ soil sample, which showed the presence of silty loam soil. The slow permeability and hydraulic conductivity range were observed by both the techniques, which also represented silty loam soil in the study area. The overall infiltration rate was less than 20 inches/h, which predicted the presence of fine-grained soil in the study area. The differences in the estimated infiltration rates at different depths reflect the differences in the recharge and precipitation.

The generated empirical equations serve as predictive tools from which bulk resistivity values could be obtained from the parameters such as pore water resistivity, porosity, and grain size measurements with good correlations obtained between these parameters. The relationships between bulk resistivity and pore water resistivity and bulk resistivity and porosity were found strong for both TEM and ERT based on the coefficient of determination. Also, validation results were in the range of the previous study, and the borehole data confirmed the presence of fine to medium-grained soil in the study area. The overall conclusion is that both geo-electrical methods worked well and have different capacities in the estimation of the hydrological parameter within the study area.

ACKNOWLEDGEMENTS

We gratefully acknowledge the Malaysian Meteorological Department, Department of Irrigation and Drainage, Malaysia, School of Physics, School of Industrial Technology,

School of Civil Engineering of Universiti Sains Malaysia, and Department of Geoscience, Universiti Teknologi PETRONAS for providing the required research facilities, University fellowship, and data for this work. We would also like to acknowledge the University of Malaya for providing financial support through the grant GPF017B-2018 to carry out this work. Furthermore, we are also many thankful to Universiti Malaysia Kelantan for the financial support to publish this work.

REFERENCES

Afshar, A, Abedi, M, Norouzi, G.H. and Riahi, M.A. 2015. Geophysical investigation of underground water content zones using electrical resistivity tomography and ground-penetrating radar: A case study in Hesarak-Karaj, Iran. Eng. Geol., 196: 183-193.

Al-Garni, M.A. and El-Kaliouby, H.M. 2011. Delineation of saline groundwater and seawater intrusion zones using transient electromagnetic (TEM) method, Wadi Thuwal area, Saudi Arabia. Arab. J. Geosci., 4(3-4): 655-668.

Anees, M.T., Abdullah, K., Nawawi, M., Ab Rahman, N.N.N., Piah, A.R.M., Syakir, M., Omar, A.M. and Hossain, K. 2017. Applications of remote sensing, hydrology, and geophysics for flood analysis. Indian J. Sci. Technol., 10(17): 450.

Archie, G.E. 1942. The electrical resistivity log is an aid in determining some reservoir characteristics. Trans. AIME, 146(01): 54-62.

Bear, J. 2013. Dynamics of Fluids in Porous Media. Courier Corporation.

Bohne, K., Nitsche, C. and Leij, F. 1989. Requirements and use of indirect methods for estimating the hydraulic functions of unsaturated soils. Paper presented in the Proceedings of the International Workshop on Indirect Methods for Estimating the Hydraulic Properties of Unsaturated Soils, eds. MT van Genuchten, FJ Leij and L]. Lund.

Bouyoucos, G.J. 1962. Hydrometer method improved for making particle size analyses of soils. Agro. J., 54(5): 464-465.

Brouwer, C., Prins, K., Kay, M. and Heibloem, M. 1988. Irrigation water management: Irrigation methods. Training Manual, p. 9.

Brunet, P., Clément, R. and Bouvier, C. 2010 Monitoring soil water content and deficit using Electrical Resistivity Tomography (ERT): A case study in the Cevennes area, France. J. Hydrol., 380(1): 146-153.

Cameron, K.C. and Buchan, G.D. 2017. Porosity: Pore Size Distribution. In Chesworth, W. (ed.), Encyclopedia of Soil Science, CRC Press, London, pp. 1782-1785.

Chen, L., Xiang, L., Young, M.H., Yin, J., Yu, Z. and Genuchten, M.T. 2015. Optimal parameters for the Green-Ampt infiltration model under rainfall conditions. J. Hydrol. Hydromech., 63(2): 93-101.

Chen, W., Huang, C., Chang, M., Chang, P. and Lu, H. 2013. The impact of floods on infiltration rates in a disconnected stream. Water Resour. Res., 49(12): 7887-7899.

Choo, H, Song, J, Lee, W. and Lee, C. 2016. Effects of clay fraction and pore water conductivity on electrical conductivity of sand-kaolinite mixed soils. J. Petrol. Sci. Eng., 147: 735-745.

Chou, T. K., Chouteau, M. and Dubé, J. S. 2016. Estimation of saturated hydraulic conductivity during infiltration test with the aid of ERT and level-set method. Vadose Zone Journal, 15(7):1-19.

Chrétien, M., Lataste, J., Fabre, R. and Denis, A. 2014. Electrical resistivity tomography to understand clay behavior during seasonal water content variations. Eng. Geol., 169: 112-123.

Crosbie, R.S., Taylor, A.R., Davis, A.C., Lamontagne, S. and Munday, T. 2014. Evaluation of infiltration from losing-disconnected rivers using a geophysical characterization of the riverbed and a simplified infiltration model. J. Hydrol., 508: 102-113.

Cui, Y.F., Zhou, X.J. and Guo, C.X. 2017. Experimental study on the moving characteristics of fine grains in wide grading unconsolidated soil under heavy rainfall. J. Mount. Sci., 14(3): 417-431.

Danielsen, J.E., Auken, E., Jørgensen, F., Søndergaard, V. and Sørensen, K.I. 2003. The application of the transient electromagnetic method in hydrogeophysical surveys. J. Appl. Geophys., 53(4): 181-198.

Das, B.M. 2013. Advanced Soil Mechanics. Fourth edition. CRC Press, London.

Dumont, G., Pilawski, T., Dzaomuho-Lenieregue, P., Hiligsmann, S., Delvigne, F., Thonart, P., Robert, T., Nguyen, F. and Hermans, T. 2016. Gravimetric water distribution assessment from geoelectrical methods (ERT and EMI) in the municipal solid waste landfill. Waste Manag., 55: 129-140.

Eluwole, A.B., Olorunfemi, M.O. and Ademilua, O.L. 2018. Soil horizon mapping and textural classification using micro soil electrical resistivity measurements: A case study from Ado-Ekiti, southwestern Nigeria. Arab. J. Geosci., 11(315): 1-11.

Fatehnia, M., Paran, S., Kish, S. and Tawfiq, K. 2016. Automating double-ring infiltrometer with an Arduino microcontroller. Geoderma, 262: 133-139.

Firdaus, M.A.R. 2018. Site Suitability Mapping for Riverbank Filtration Using Spatial Analysis of Surface And Subsurface Characteristic. Ph.D., School of Civil Engineering, Universiti Sains Malaysia, Pulau Penang, Malaysia.

Flores, C., Romo, J.M. and Vega, M. 2013. On the estimation of the maximum depth of investigation of transient electromagnetic soundings: the case of the Vizcaino transect, Mexico. Geof. Int., 52(2): 159-172.

Freeze, A.R., and Cherry, J.A. 1979. Groundwater. Prentice-Hall International, INC., Englewood Cliffs, New Jersey.

Ghose, R. and Slob, E. 2006. Quantitative integration of seismic and GPR reflections to derive unique estimates for water saturation and porosity in the subsoil. Geophys. Res. Lett., 33(5): 1-4.

Green, W.H. and Ampt, G. 1911. Studies on soil physics. J. Agric. Sci., 4(1): 1-24.

Heng, G.S., Hoe, T.G. and Hassan, W.F.W. 2006. Gold mineralization and zonation in the State of Kelantan. Geol.Soc. Malaysia Bull., 52: 129-135.

Kozeny, J. 1953. Hydraulics. Springer-Verlag, Wien.

Kumar, D., Mondal, S., Nandan, M., Harini, P., Sekhar, B.S. and Sen, M.K. 2016. Two-dimensional electrical resistivity tomography (ERT) and time-domain-induced polarization (TDIP) study in hard rock for groundwater investigation: a case study at Choutuppal Telangana, India. Arab. J. Geosci., 9(5): 355.

Li, B. and Sherman, D.J. 2015. Aerodynamics and morphodynamics of sand fences: A review. Aeol. Res., 17: 33-48.

Maidment, D. R. 1993. Handbook of Hydrology. Volume 1. McGraw-Hill, New York.

Morbidelli, R., Saltalippi, C., Flammini, A., Cifrodelli, M., Corradini, C. and Govindaraju, R.S. 2015. Infiltration on sloping surfaces: Laboratory experimental evidence and implications for infiltration modeling. J. Hydrol., 523: 79-85.

Morel-Seytoux, H.J., Meyer, P.D., Nachabe, M., Tourna, J., Genuchten, M.V. and Lenhard, R.J. 1996. Parameter equivalence for the Brooks-Corey and van Genuchten soil characteristics: Preserving the effective capillary drive. Water Resour. Res., 32(5): 1251-1258. https://doi.org/10.1029/96WR00069

Niwas, S. and Celik, M. 2012. Equation estimation of porosity and hydraulic conductivity of Ruhrtal aquifer in Germany using near-surface geophysics. J. Appl. Geophys., 84: 77-85.

Noell, U., Wießner, C., Ganz, C. and Westhoff, M. 2011. Direct observations of surface water-groundwater interaction using electrical resistivity tomography. In Symposium H01 on Conceptual and Modelling Studies of Integrated Groundwater, Surface Water, and Ecological Systems, Held During the 25th General Assembly of the International Union of Geodesy and Geophysics, IUGG 93, pp. 42-47.

Palacky, G. 1988. Resistivity characteristics of geologic targets. Soc. Explor. Geophys., 1: 53-129.

Perrone, A., Lapenna, V. and Piscitelli, S. 2014. Electrical resistivity tomography technique for landslide investigation: a review. Earth-Sci. Rev., 135: 65-82.

Saarenketo, T. 1998. Electrical properties of water in clay and silty soils. J. Appl. Geophys., 40(1-3): 73-88.

Shaari, N.A., Ali, K.M.M. and Mukhtar, A. 2016. Estimation of infiltration rate in major soil types of Kota Bharu, Kelantan, Malaysia. Bull. Geol. Soc. Malay., 62: 7-11.

Shepherd, R.G. 1989. Correlations of permeability and grain size. Groundwater, 27(5): 633-638.

Todd, D.K. and Mays, L. 1980. Groundwater Hydrogeology. John Willey and Sons Inc., New York.

Turesson, A. 2006. Water content and porosity are estimated from ground-penetrating radar and resistivity. J. Appl. Geophys., 58(2): 99-111.

Vaezi, A.R., Hasanzadeh, H. and Cerdà, A. 2016. Developing an erodibility triangle for soil textures in semi-arid regions, NW Iran. Catena, 142: 221-232.

Van Genuchten, M.T. 1980. A closed-form equation for predicting the hydraulic conductivity of unsaturated soils. Soil Sci. Soc. Am. J., 44(5): 892-898.